

Determination of the neutron skin of atomic nuclei

Xavier Roca Maza
Università degli studi di Milano & INFN

Nuclear physics confronts relativistic collisions of isobars

Heidelberg, May 30th to June 3rd, 2022

Table of contents

How we can directly measure the point neutron and proton density distributions model independently?

Elastic electron scattering and parity violating electron scattering; access to the isotope shift in charge radii also via laser spectroscopy.

Implications for nuclear structure from precision neutron skin measurements (or indirect measurements of the neutron skin)

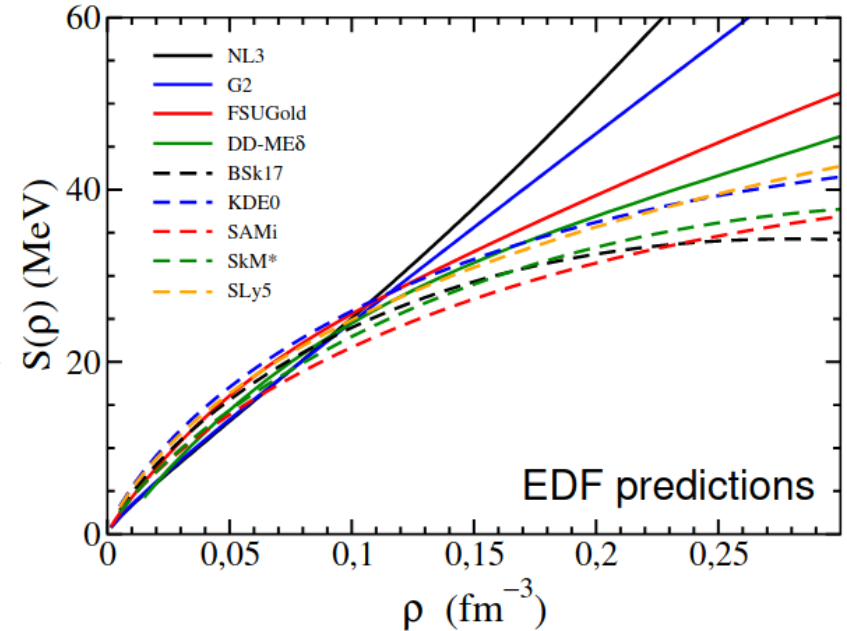
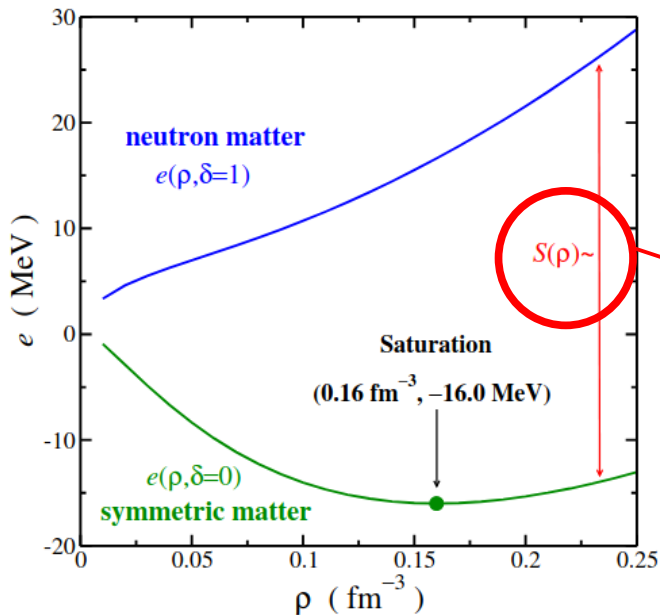
Atomic parity violation and BSM, Dipole polarizability, Giant Dipole and Quadrupole resonances and their low lying strength, Isobaric Analog State, Charge radii in mirror nuclei, Spin Dipole Resonance ...

Implications for nuclear astrophysics from precision neutron skin measurements.

Nuclear Equation of State, Mass-Radius relation and deformability of a (light) neutron star, Composition of the crust of a neutron star ...

Nuclear Equation of State

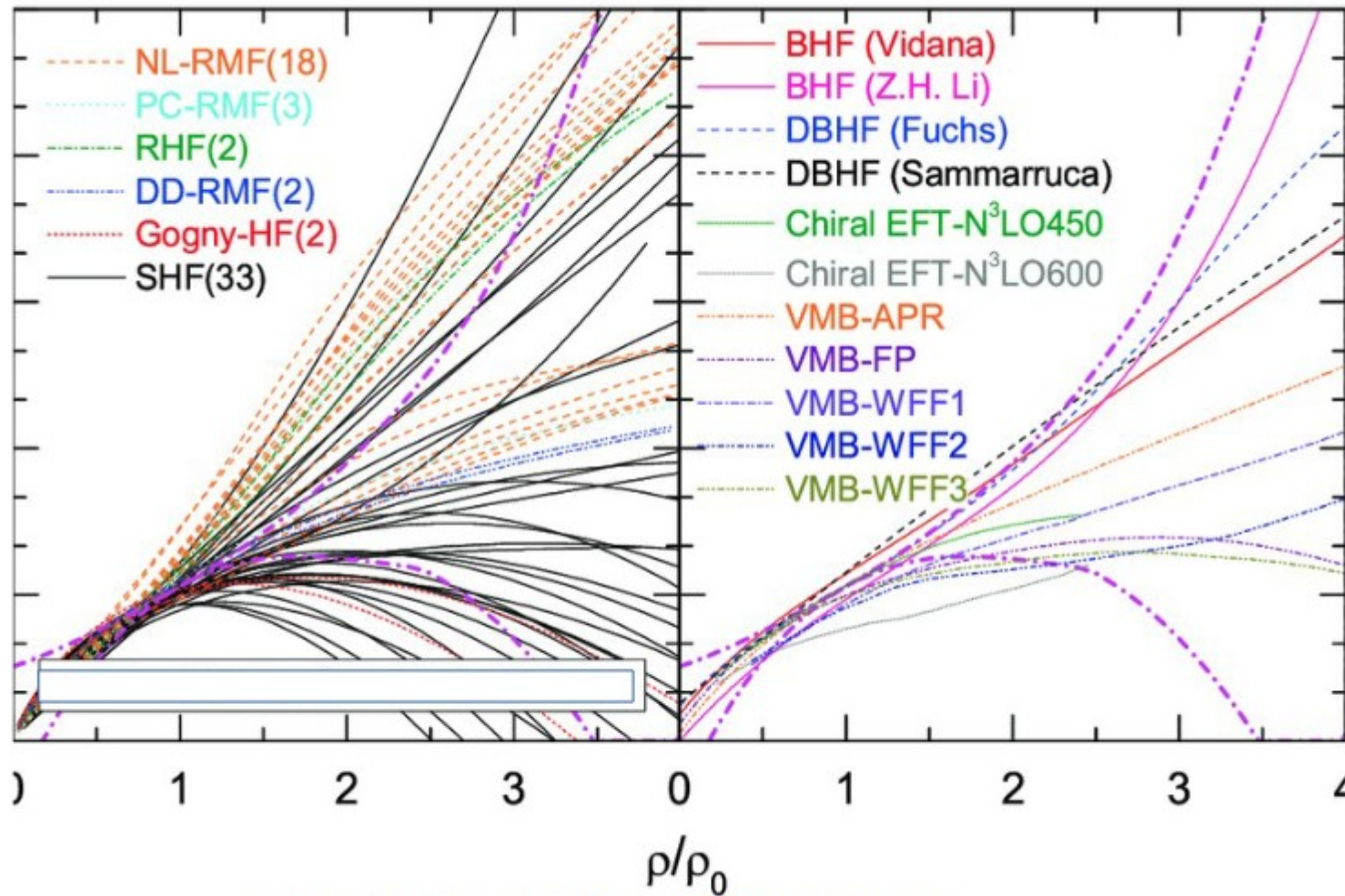
-**Isvector properties** not well determined in current **EDFs**



$$e(\rho, \beta) = e(\rho, \beta = 0) + S(\rho)\beta^2 + \mathcal{O}(\beta^4) \quad \text{where } \beta \equiv \frac{\rho_n - \rho_p}{\rho}$$

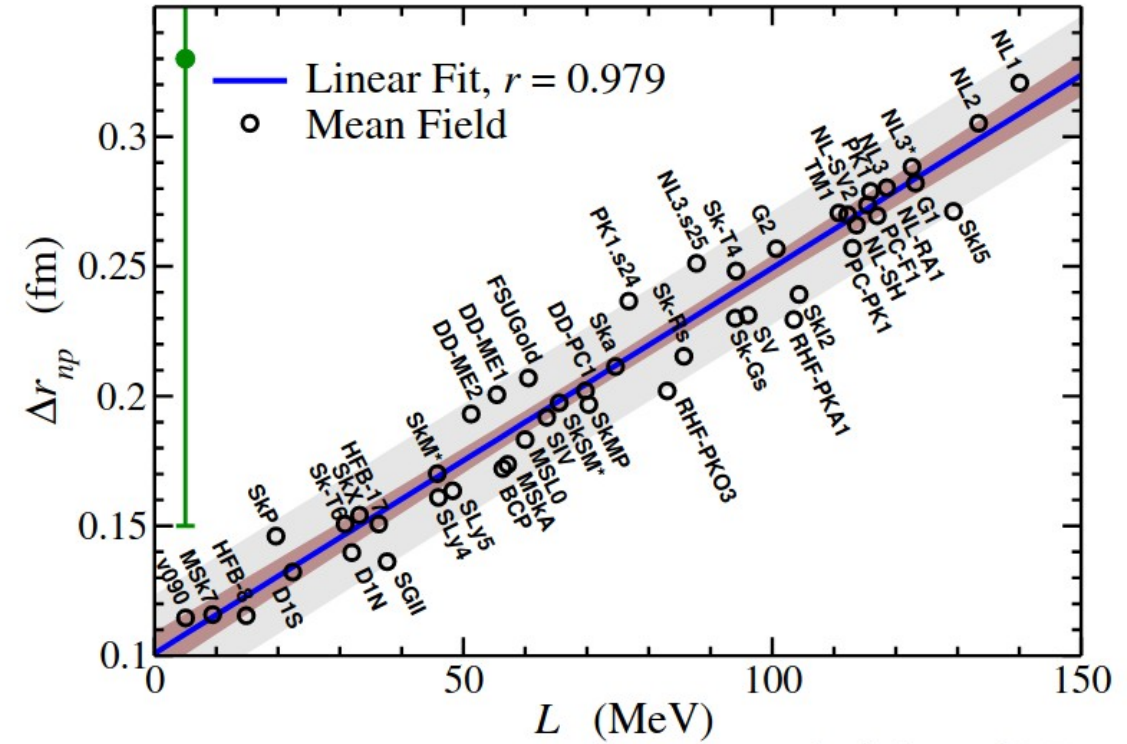
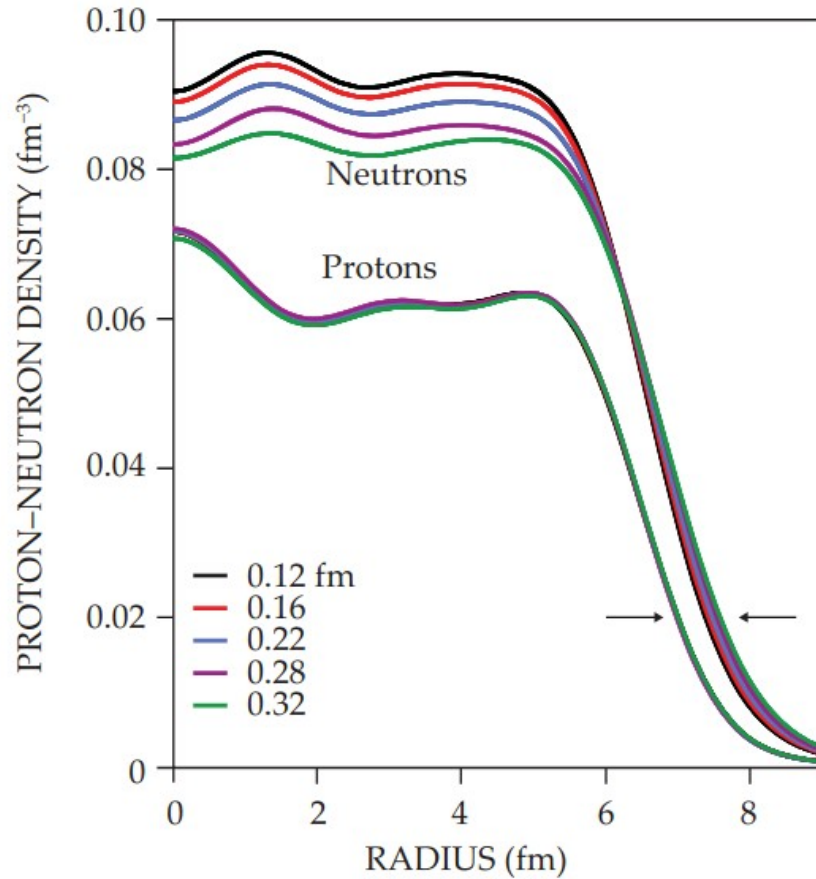
$$\text{where } J \equiv S(\rho_0) \text{ and } L \equiv 3\rho_0 \left. \frac{\partial S}{\partial \rho} \right|_{\rho_0} = 3\rho_0 p_0^{\text{neut}}$$

Nuclear Equation of State



Towards understanding astrophysical effects of nuclear symmetry energy
Bao-An Li, Plamen G. Krastev, De-Hua Wen & Nai-Bo Zhang EPJ A 55, 117 (2019)

Neutron skin thickness



$$\Delta r_{np} \equiv \langle r_n^2 \rangle^{1/2} - \langle r_p^2 \rangle^{1/2} \sim \frac{1}{12} \frac{N-Z}{A} \frac{R}{J} L$$

Physics Today **72**, 7, 30 (2019)

X. Roca-Maza, M. Centelles, X. Viñas, and M. Warda
Phys. Rev. Lett. **106**, 252501 (2011) - Published 21 June 2011

Elastic electron scattering: $\rho_{\text{ch}} \rightarrow \rho_{\text{p}}$

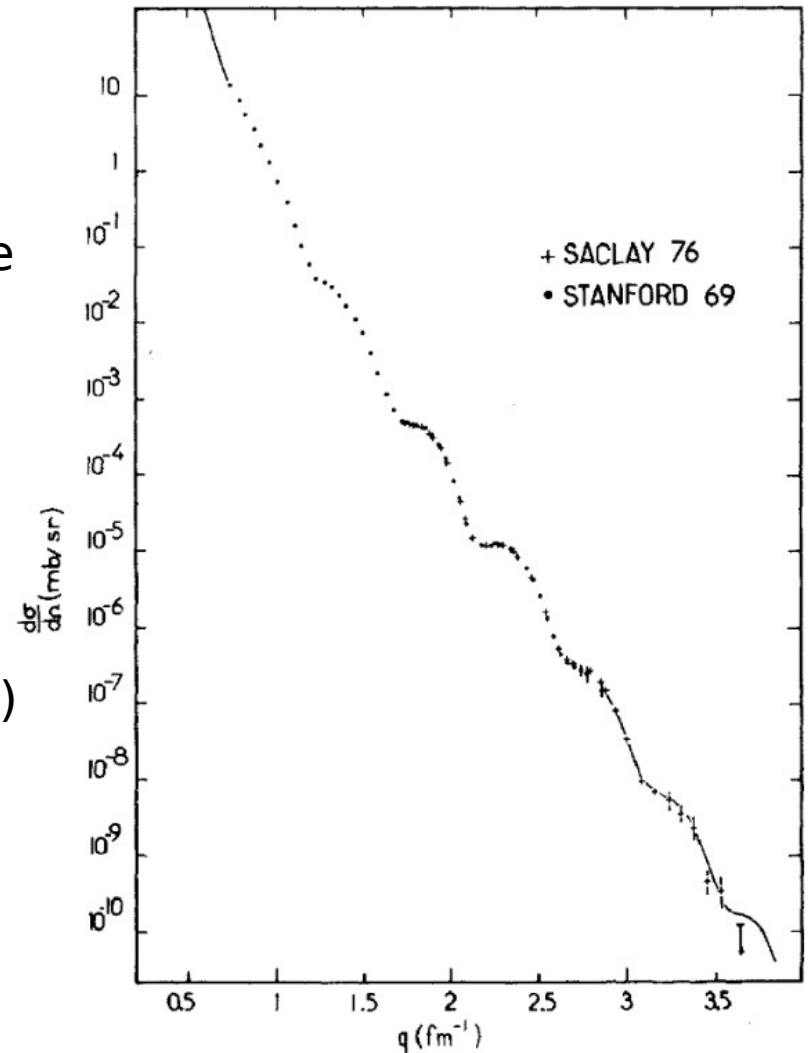
$$E_{\text{beam}} \sim \frac{2\pi\hbar c}{\lambda_{\text{nuclear}}} \sim 10^2 \text{MeV}$$

The **scattering of relativistic electrons** by the **Coulomb field** $V(r)$ is completely **described** by the direct scattering amplitude, $\mathbf{f}(\boldsymbol{\theta})$, and the spin-flip scattering amplitude, $\mathbf{g}(\boldsymbol{\theta})$.

$$\frac{d\sigma}{d\Omega} = |f(\theta)|^2 + |g(\theta)|^2$$

$f(\theta)$ and $g(\theta)$ determined from the **solutions of the Dirac equation** for the central potential $V(r)$

$$V_{\text{nucl.elec.}} = 4\pi Z_0 e^2 \left\{ \frac{1}{r} \int_0^r \rho_{\text{ch}}(u) u^2 du + \int_r^\infty \rho_{\text{ch}}(u) u du \right\}$$



Elastic electron scattering: $\rho_{ch} \rightarrow \rho_p$

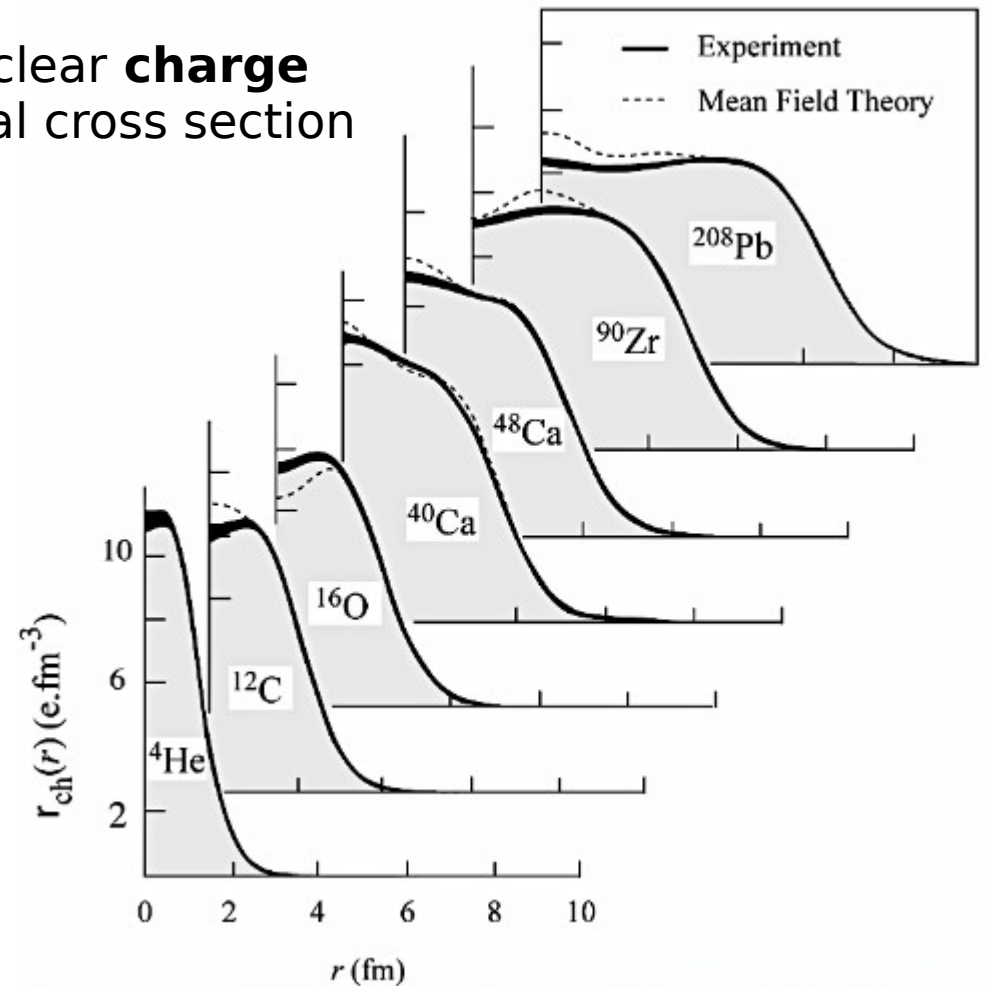
Experimentally one can access the nuclear **charge form factor** dividing by the differential cross section of a point nucleus with charge Z

$$\frac{d\sigma}{d\Omega} = \left(\frac{d\sigma}{d\Omega} \right)_{\text{Mott}} |F(q)|^2$$

The low momentum transfer behavior of the form factor determines the **charge radius**

$$F_{ch}(q) = Z \left(1 + \frac{q^2 \langle r_{ch}^2 \rangle}{3!} + [O]q^4 \right)$$

The **Fourier transform** of $F_{ch}(q)$ gives access to $\rho_{ch}(r)$.

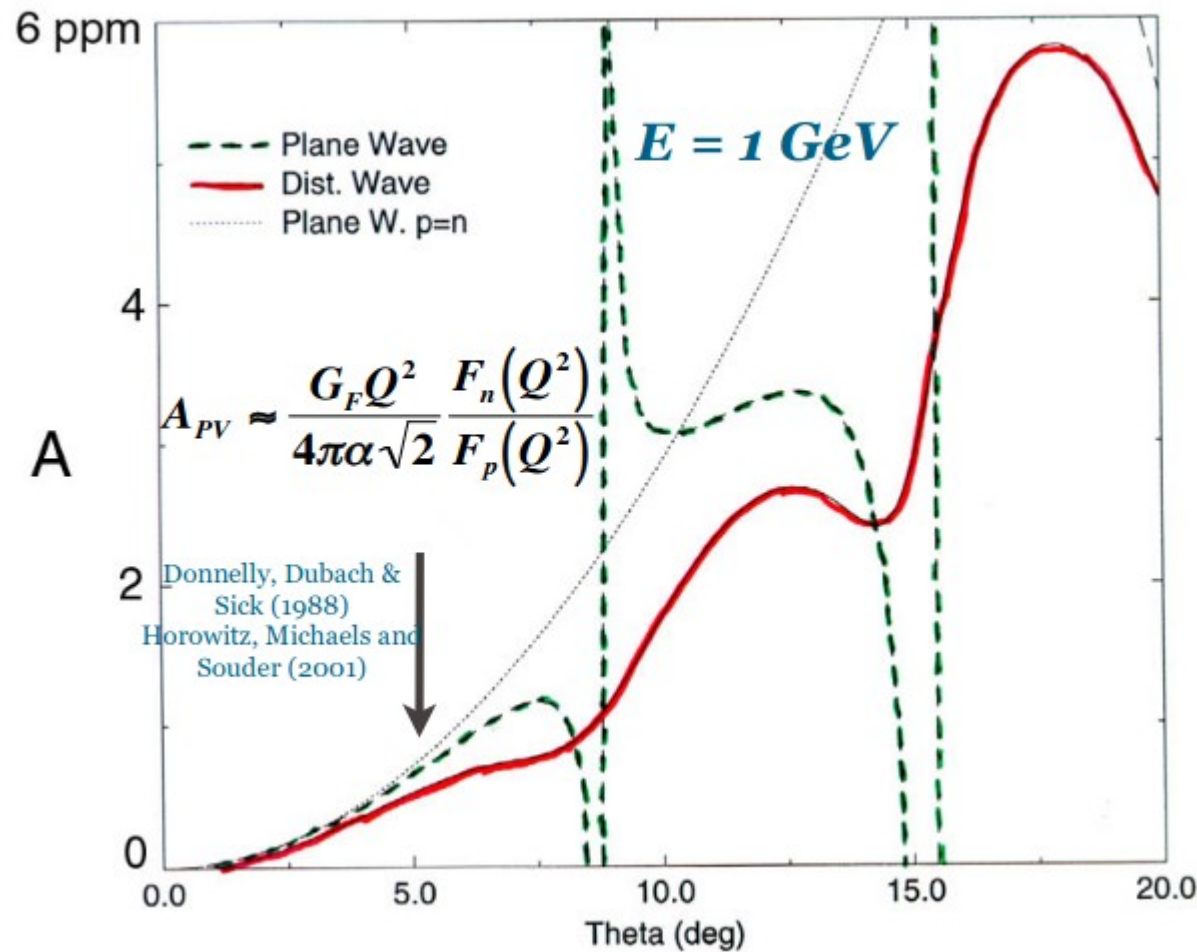


Parity Violating electron elastic scattering: $\rho_w \rightarrow \rho_n$

- ▶ **Electrons** interact by exchanging a γ or a Z_0 boson.
- ▶ While **protons** couple basically to γ , **neutrons** do it to Z_0 .
- ▶ **Ultra-relativistic electrons**, depending on their helicity, interact with the nucleons $V_{\pm} = V_{\text{Coulomb}} \pm V_{\text{Weak}}$.
- ▶ **Ultra-relativistic electrons** moving under the effect of V_{\pm} where **Coulomb distortions** are important \Rightarrow solution of the Dirac equation via the Distorted Wave Born Approximation (**DWBA**).
- ▶ **Input for the calculation:** ρ_n and ρ_p (as well as nucleon electromagnetic and weak form factors)

$$A_{\text{pv}} = \left(\frac{d\sigma_+}{d\Omega} - \frac{d\sigma_-}{d\Omega} \right) / \left(\frac{d\sigma_+}{d\Omega} + \frac{d\sigma_-}{d\Omega} \right)$$

Parity Violating electron elastic scattering: A_{pv} at the PREx kinematics



$F_{ch}(\mathbf{q})$ and $A_{pv}(\mathbf{q})$ if measured at different \mathbf{q} allow to **determine** $\rho_{ch}(\mathbf{r})$ and $\rho_w(\mathbf{r})$

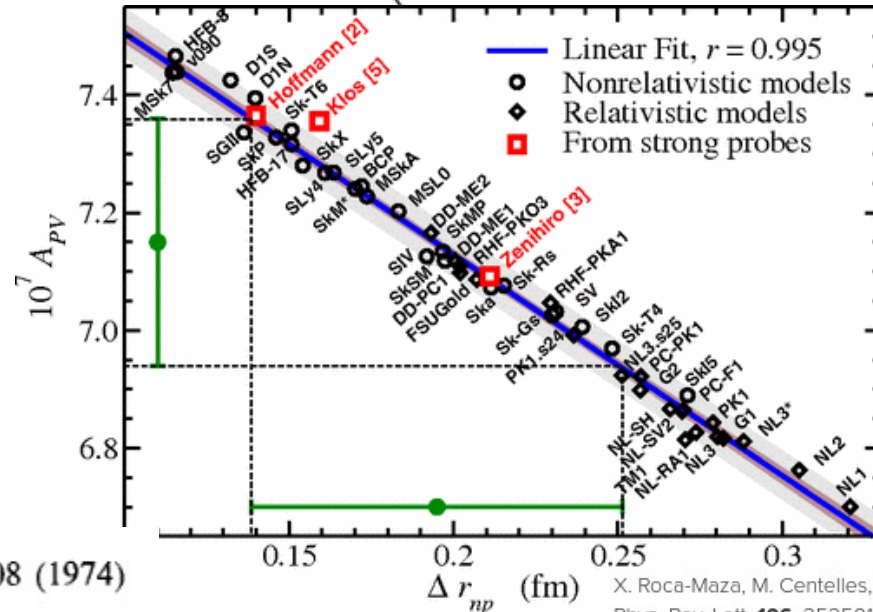
Current situation (^{208}Pb)

While $\rho_{\text{ch}}(\mathbf{r})$ has been **determined** in **different nuclei**, $\rho_{\text{w}}(\mathbf{r})$ has **not** been **determined** since A_{pv} has only been measured at a **single q** for ^{208}Pb and ^{48}Ca

| nucleus | ^{206}Pb | | ^{208}Pb | |
|-----------------------------|-------------------|----------|------------------------|----------|
| rms [fm] | 5.490 | | 5.503(2) | |
| i | R_i | Q_i | R_i | Q_i |
| 1 | 0.6 | 0.010615 | 0.1 | 0.003845 |
| 2 | 1.1 | 0.021108 | 0.7 | 0.009724 |
| 3 | 2.1 | 0.000060 | 1.6 | 0.033093 |
| 4 | 2.6 | 0.102206 | 2.1 | 0.000120 |
| 5 | 3.1 | 0.023476 | 2.7 | 0.083107 |
| 6 | 3.8 | 0.065884 | 3.5 | 0.080869 |
| 7 | 4.4 | 0.226032 | 4.2 | 0.139957 |
| 8 | 5.0 | 0.000005 | 5.1 | 0.260892 |
| 9 | 5.7 | 0.459690 | 6.0 | 0.336013 |
| 10 | 6.8 | 0.086351 | 6.6 | 0.033637 |
| 11 | 7.2 | 0.004589 | 7.6 | 0.018729 |
| 12 | 8.6 | 0.000011 | 8.7 | 0.000020 |
| ref. | Fr83 | | Fr77a | |
| q-range [fm ⁻¹] | 0.51- 2.99 | | 0.44- 3.70 | |
| data-sets | Eu78,Fr83 | | He69,Ni69, Eu76a,Fr77a | |
| RP [fm] | 1.70 | | 1.70 | |

In PWBA for small momentum transfer:

$$A_{\text{pv}} \approx \frac{G_F q^2}{4\sqrt{2}\pi\alpha} \left(1 - \frac{q^2 \langle r_p^2 \rangle^{1/2}}{3F_p(q)} \Delta r_{\text{np}} \right)$$



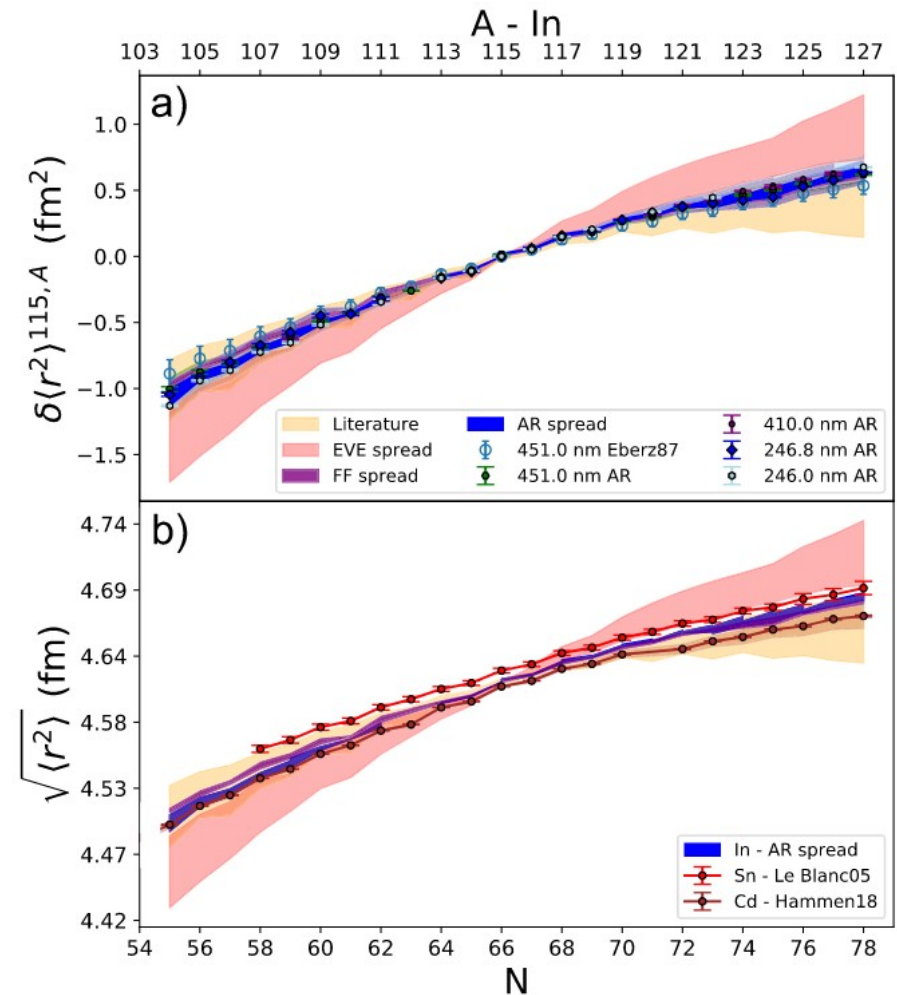
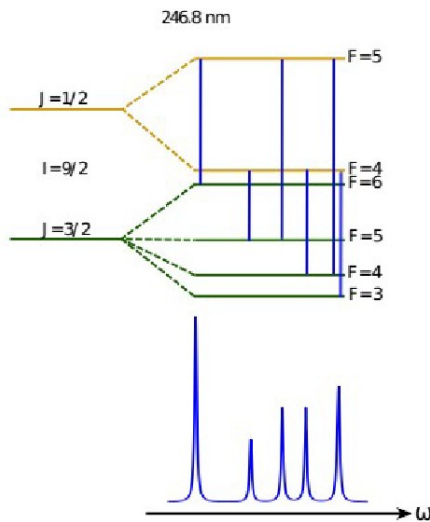
ATOMIC DATA AND NUCLEAR DATA TABLES 14, 479–508 (1974)

X. Roca-Maza, M. Centelles, X. Viñas, and M. Warda
 Phys. Rev. Lett. **106**, 252501 (2011) - Published 21 June 2011

Laser spectroscopy: hyperfine structure

→ **Atomic energy levels** are **split** by the interaction of atomic electrons with the **nuclear magnetic dipole moment** and by **nuclear electric quadrupole moment**

→ **Isotope shifts** give changes in mean square charge radii $\delta\langle r_{ch}^2 \rangle$



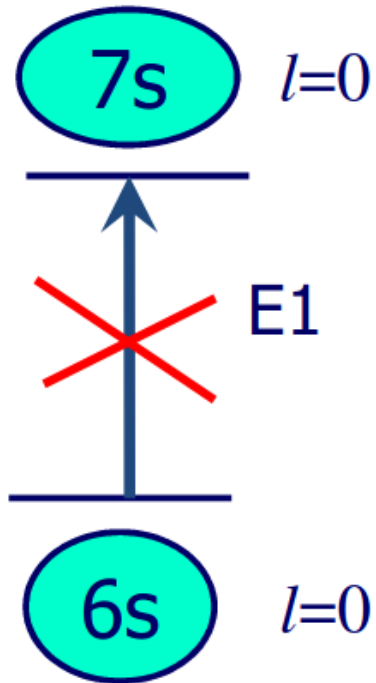
B K Sahoo et al 2020 *New J. Phys.* **22** 012001

Implications for nuclear structure from precision neutron skin measurements

- Atomic parity non conservation (Q_w and R_w)
- Neutrino coherent [$F(q \rightarrow 0) \rightarrow 1$] elastic scattering (Q_w and R_w)
- Dipole polarizability (J , Δr_{np})
- Isobaric Analog State (V_{ISB} , Δr_{np})
- Spin Dipole Resonance (Δr_{np} , ...)
- Charge radii in mirror nuclei (Δr_{np}) [?]
- Giant Dipole and Quadrupole resonances (Δr_{np} , ...)
- Among other observables !!

Atomic parity non conservation

Cs atom



Transition allowed only by **parity violation**, otherwise forbidden

$$H_{PNC}^{(1)} = \frac{G_F}{2\sqrt{2}} Q_W \gamma_5 \rho(r)$$

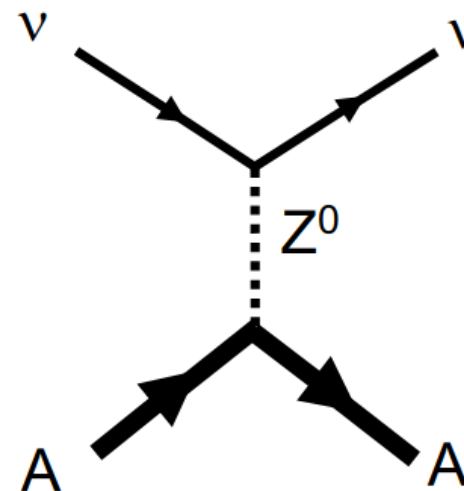
Neutron density!!

$$E_{PNC} = E_{PNC}^{theory} Q_W^{inferred}$$

RMP 90, 025008 (2018)

Coherent neutrino nucleus elastic scattering

Neutrinos with $E < 50$ MeV exchange a Z_0 boson and the nucleus recoils as a “whole”



$$\frac{d\sigma}{dT} \simeq \frac{G_F^2 M}{2\pi} \frac{Q_W^2}{4} F^2(Q) \left(2 - \frac{MT}{E_\nu^2} \right)$$

E_ν : neutrino energy
 T : nuclear recoil energy
 M : nuclear mass
 $Q = \sqrt{2MT}$:
 momentum transfer

weak nuclear charge

Form factor: $F=1 \rightarrow$ full coherence

$$Q_W = (1 - 4 \sin^2 \theta_W)Z - N$$

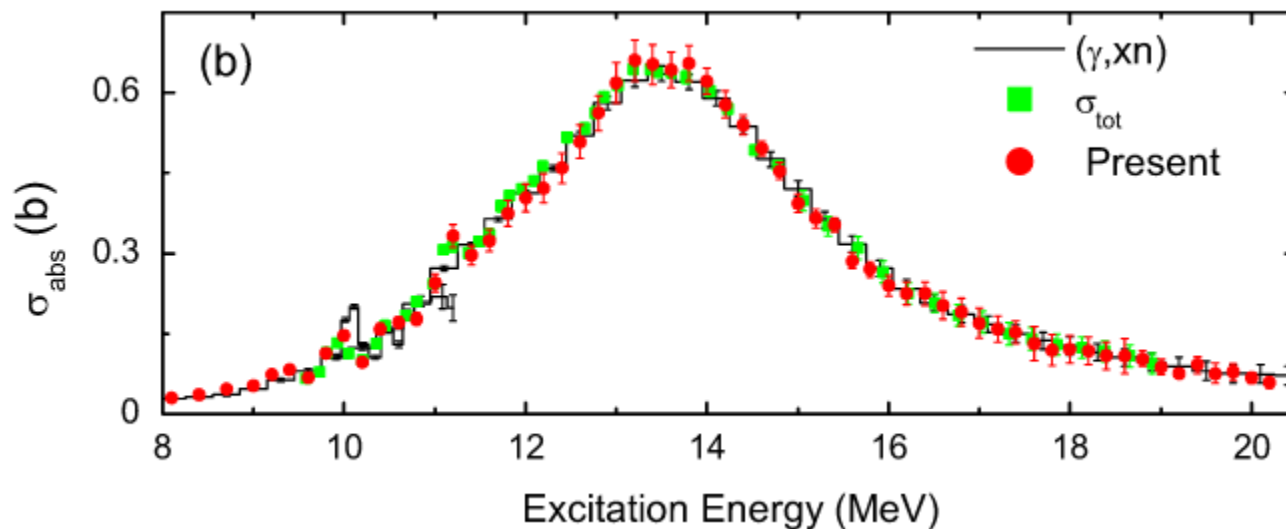
Taken from a presentation by **Kate Scholberg**, Duke University

Dipole polarizability (α_D)

The electric **polarizability** measures the tendency of the nuclear **charge distribution to be distorted**

$$\alpha_D \sim \frac{\text{electric dipole moment}}{\text{external electric field}}$$

$$\alpha_D = \frac{\hbar c}{2\pi^2} \int \frac{\sigma_{\text{ph. abs.}}(E)}{E^2} dE$$



Phys. Rev. Lett. **107**, 062502 – Published 3 August 2011

Dipole polarizability (α_D): SIMPLE MODEL

The **dielectric theorem** establishes that the m_{-1} moment can be computed from the **expectation value of the Hamiltonian in the constrained ground state** $\mathcal{H}' = \mathcal{H} + \lambda \mathcal{D}$.

Adopting the Droplet Model ($m_{-1} \propto \alpha_D$):

$$m_{-1} \approx \frac{A \langle r^2 \rangle^{1/2}}{48J} \left(1 + \frac{15}{4} \frac{J}{Q} A^{-1/3} \right)$$

Bulk - First derived by Migdal

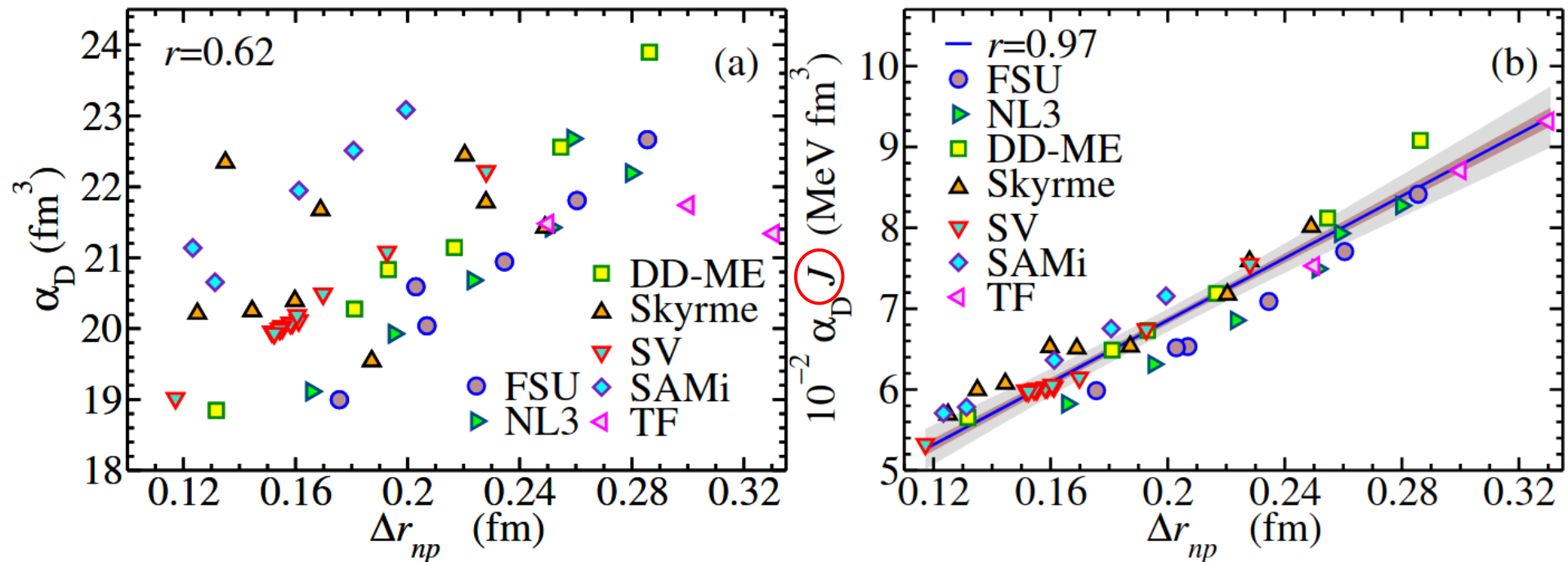
Surface correction - first derived by J. Meyer, P. Quentin, and B. Jennings, Nucl. Phys. A 385, 269 (1982)

within the same model, connection with the neutron skin thickness:

$$\alpha_D \approx \frac{A \langle r^2 \rangle}{12J} \left[1 + \frac{5}{2} \frac{\Delta r_{np} + \sqrt{\frac{3}{5}} \frac{e^2 Z}{70J} - \Delta r_{np}^{\text{surface}}}{\langle r^2 \rangle^{1/2} (I - I_C)} \right]$$

Dipole polarizability (α_D): EDFs

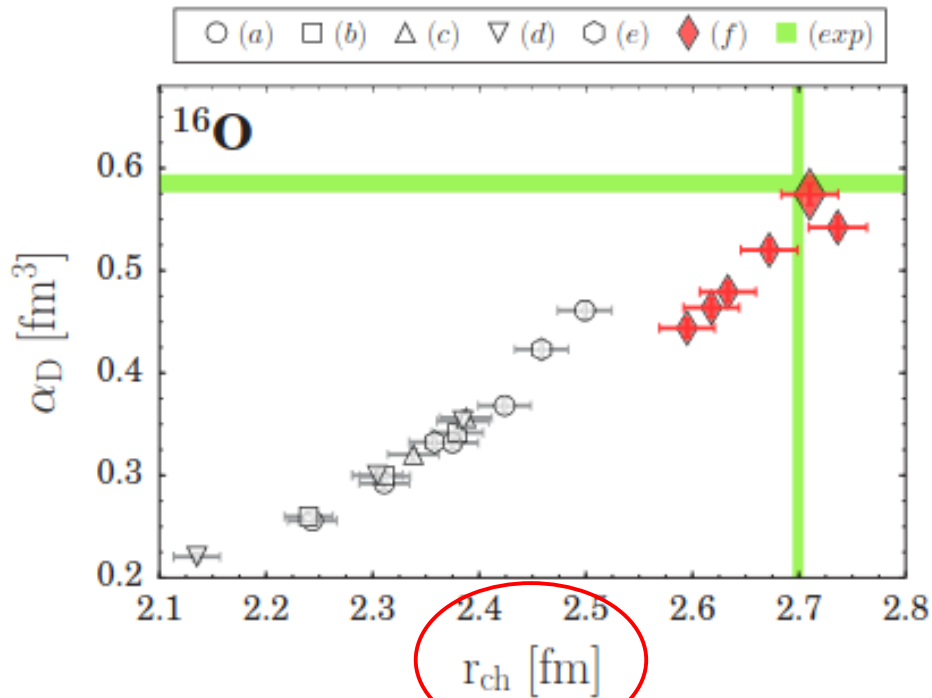
Dipole polarizability: microscopic results HF+RPA



X. Roca-Maza, *et al.*, Phys. Rev. C 88, 024316 (2013).

$\alpha_D J$ is linearly correlated with Δr_{np} and no α_D alone within EDFs

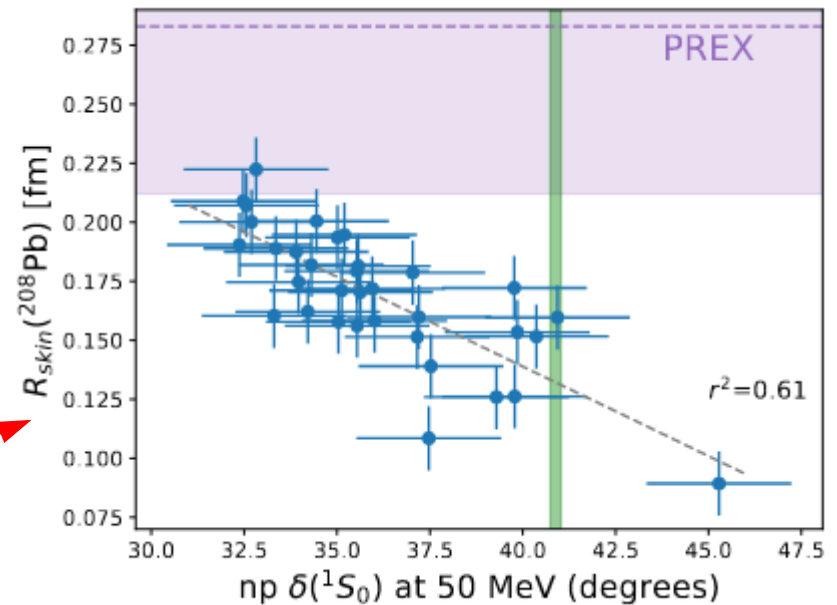
Dipole polarizability (α_D): ab initio



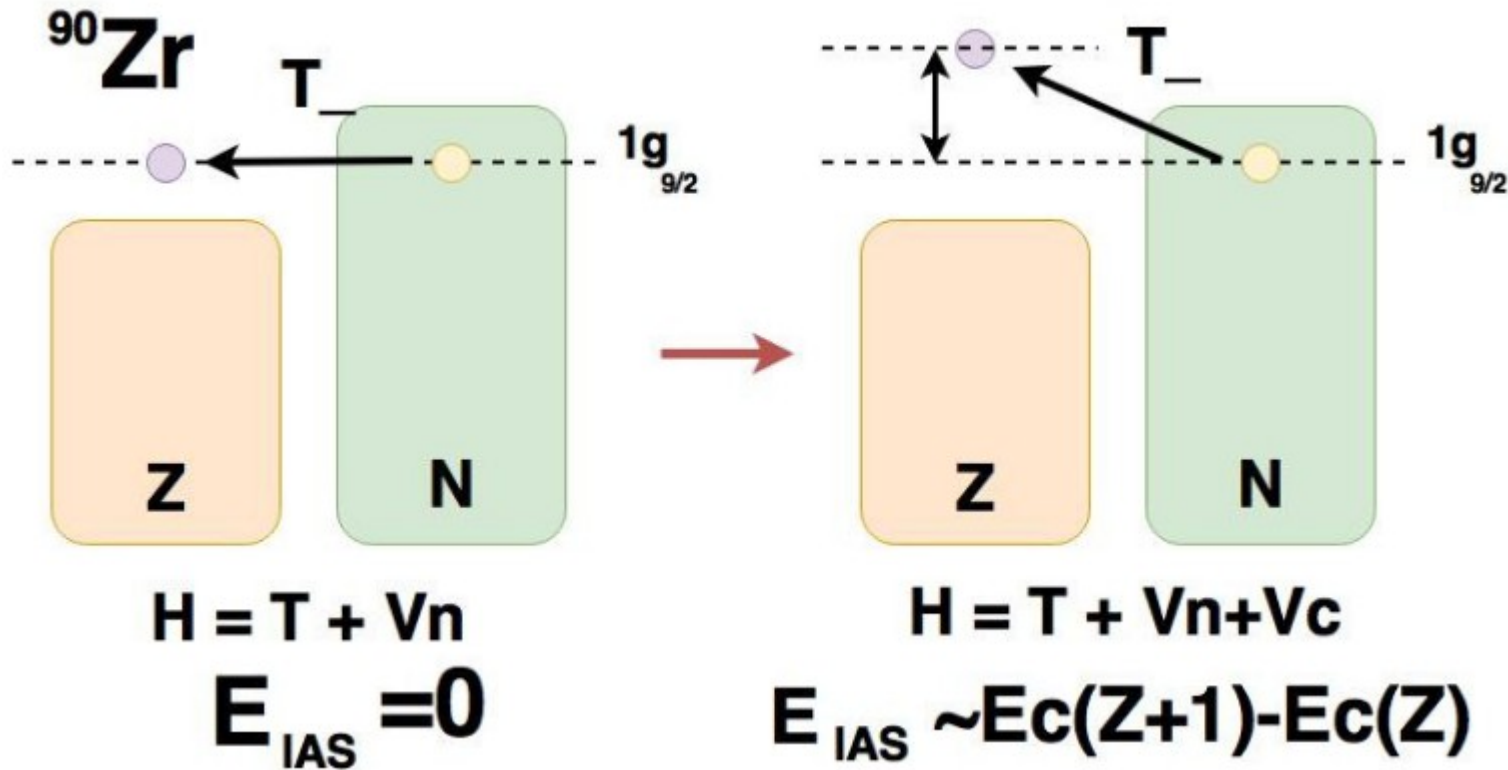
PHYSICAL REVIEW C **94**, 034317 (2016)

Dependence on R_{ch} since Δr_{np} is better determined in ab initio due to the fitting of the 1S_0 partial wave in np scattering

- (a) SRG evolved EM $\Lambda = 500$
- (b) SRG evolved EM $\Lambda = 600$
- (c) SRG evolved CD-BONN
- (d) Vlow-k evolved CD-BONN potentials
- (e) Vlow-k -evolved AV18
- (f) refer to calculations that include 3NF: The large one is from NNLOsat



Isobaric Analog State



$$E_{IAS} = E_A - E_0 = \langle A | \mathcal{H} | A \rangle - \langle 0 | \mathcal{H} | 0 \rangle = \frac{\langle 0 | T_+ [\mathcal{H}, T_-] | 0 \rangle}{\langle 0 | T_+ T_- | 0 \rangle}$$

Isobaric Analog State: SIMPLE MODEL

- Assuming independent particle model and good isospin for $|0\rangle$
($\langle 0|T_+T_-|0\rangle = 2T_0 = N - Z$)

$$E_{IAS} \approx E_{IAS}^{C,direct} = \frac{1}{N - Z} \int [\rho_n(\vec{r}) - \rho_p(\vec{r})] U_C^{direct}(\vec{r}) d\vec{r}$$

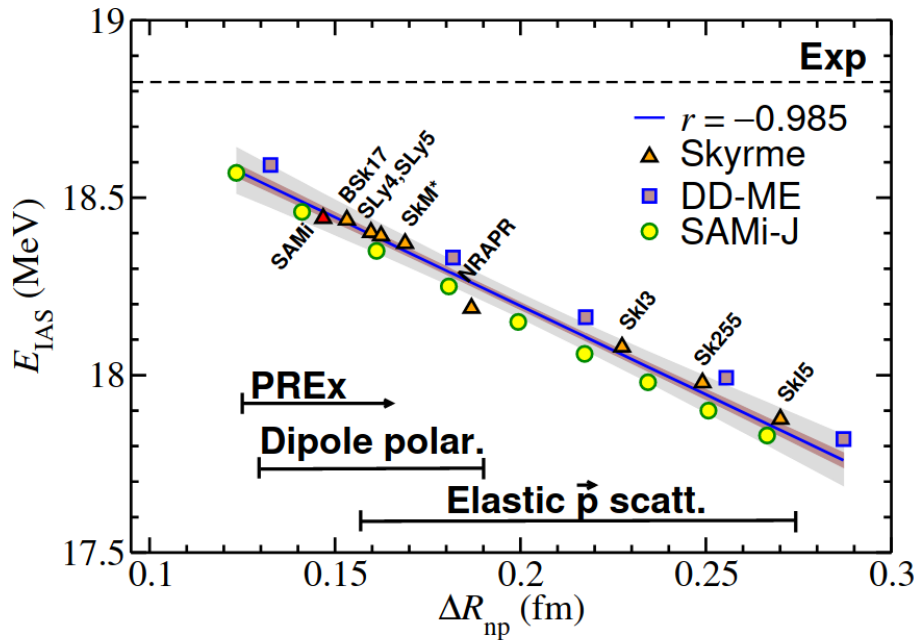
where $U_C^{direct}(\vec{r}) = \int \frac{e^2}{|\vec{r}_1 - \vec{r}|} \rho_{ch}(\vec{r}_1) d\vec{r}_1$

- Assuming also a uniform neutron and proton distributions of radius R_n and R_p respectively, and $\rho_{ch} \approx \rho_p$ one can find

$$E_{IAS} \approx E_{IAS}^{C,direct} \approx \frac{6}{5} \frac{Ze^2}{R_p} \left(1 - \sqrt{\frac{5}{12}} \frac{N}{N - Z} \frac{\Delta r_{np}}{R_p} \right)$$

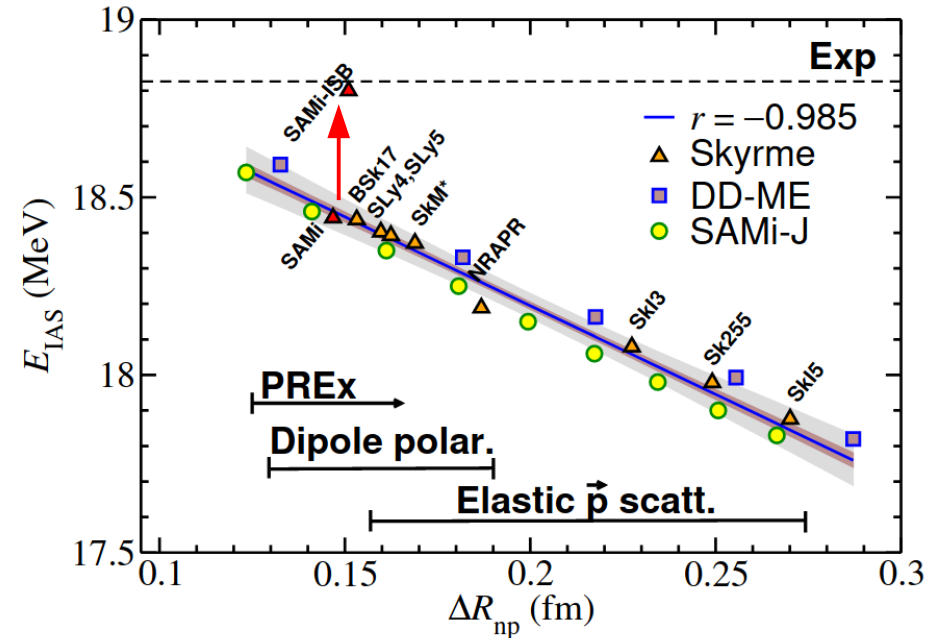
One may expect: **the larger the Δr_{np} the smallest E_{IAS}**

Isobaric Analog State: EDFs



Phys. Rev. Lett. 120, 202501 (2018)

Nuclear models (EDFs) where the nuclear part is isospin symmetric and U_{ch} is calculated from the ρ_p



Phys. Rev. Lett. 120, 202501 (2018)

Measurement of $\Delta r_{np} \rightarrow$ determine ISB in the nuclear medium

Treatment of Coulomb + QED corrections + **nuclear Isospin symmetry Breaking**

Spin-Dipole Resonance: sum rule

Excitation operator:

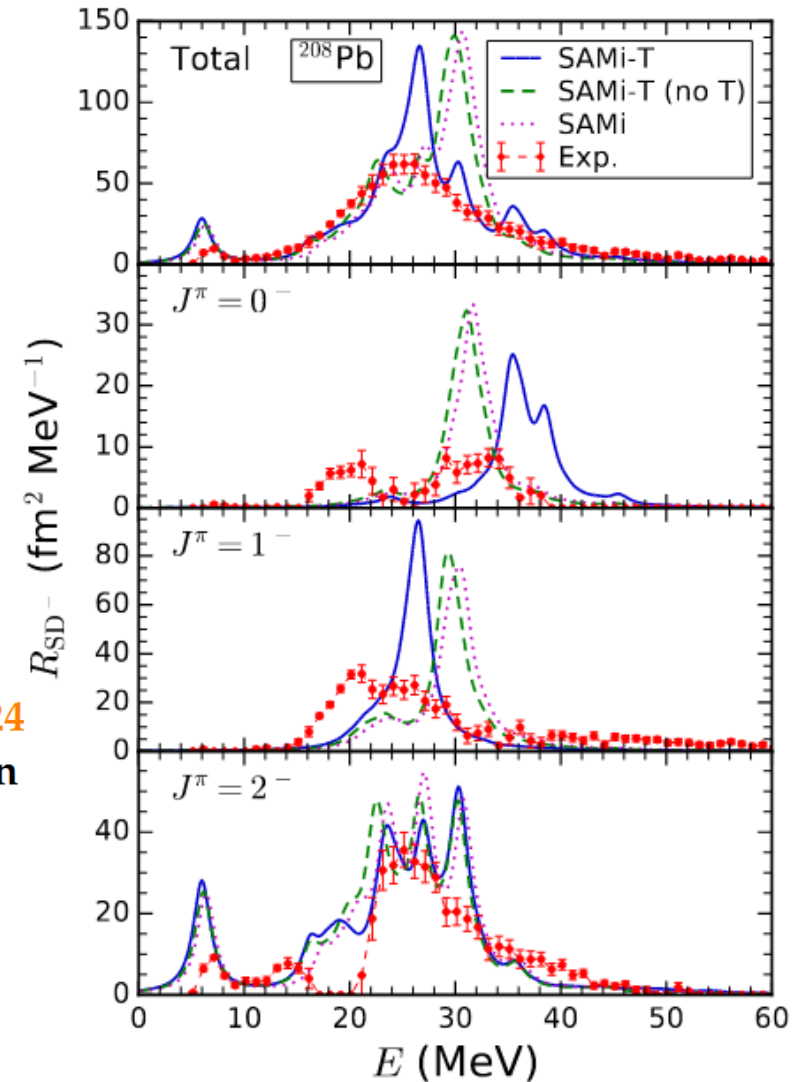
$$\hat{O}_{\text{SDR}} = \sum_{i=1}^A \sum_M \tau_{\pm}(i) r_i^L [Y_L(\hat{r}_i) \otimes \sigma(i)]_{JM}.$$

Non energy weighted sum rule:

$$\int [R_{\text{SD}^-}(E) - R_{\text{SD}^+}(E)] dE = \frac{9}{4\pi} (N \langle r_n^2 \rangle - Z \langle r_p^2 \rangle) \\ \approx (N - Z) \langle r_p^2 \rangle \left(1 + \frac{2N}{N - Z} \frac{\Delta r_{\text{np}}}{\langle r_p^2 \rangle^{1/2}} \right)$$

- Experimental NEWSR in ^{208}Pb is $1004^{+24}_{-23} \text{ fm}^2$; SAMi is 1224 fm^2 ; and SAMi-T $1260 \pm 10 \text{ fm}^2$ (some strength is missing in the experimental measurement? $\Delta r_{\text{np}} \approx 0.05 \text{ fm}$).
- Experimental NEWSR in ^{90}Zr is $148 \pm 12 \text{ fm}^2$; SAMi is 150 fm^2 ; and SAMi-T $147 \pm 1 \text{ fm}^2 \Rightarrow$ neutron skin should be properly determined by SAMi and SAMi-T

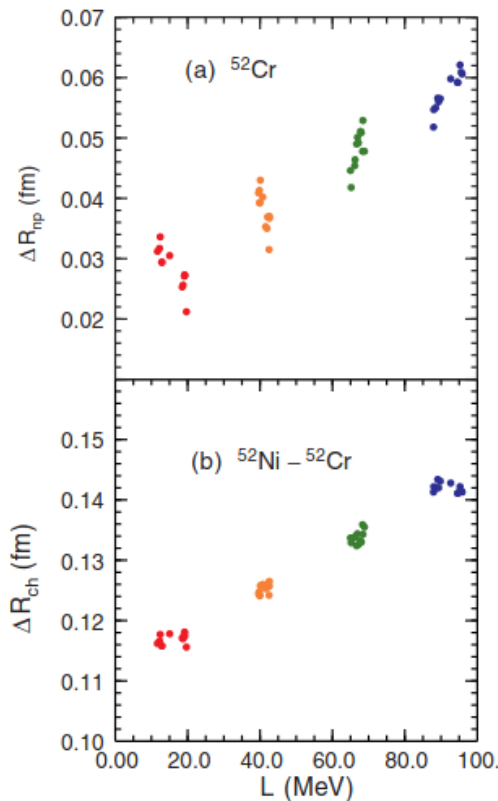
Shihang Shen (申时行), Gianluca Colò, and Xavier Roca-Maza
Phys. Rev. C **99**, 034322 – Published 20 March 2019



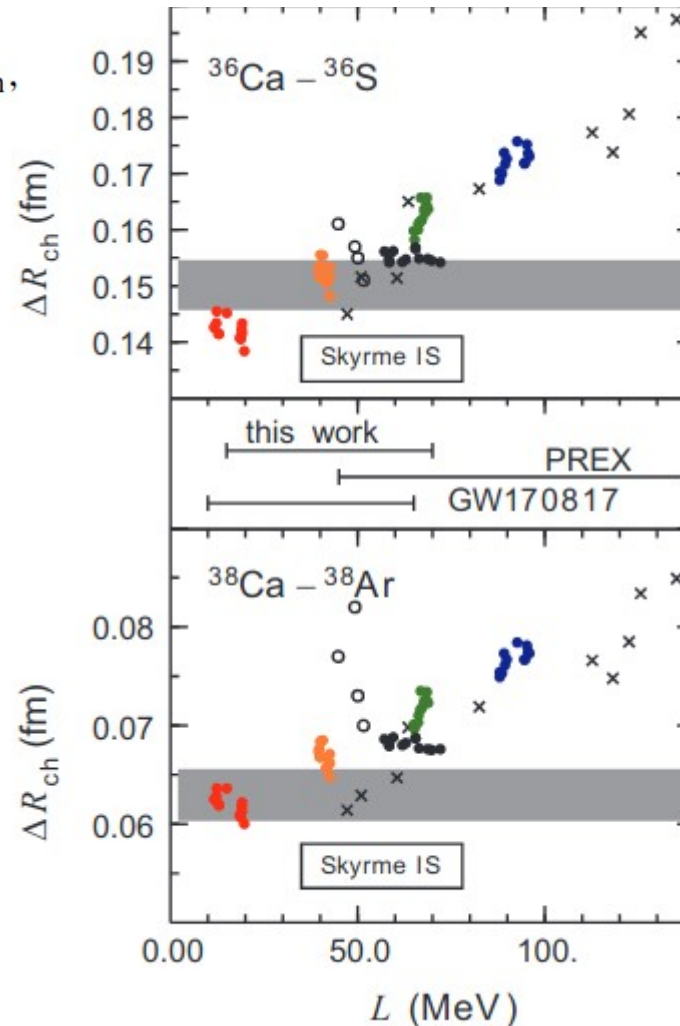
Charge radii in mirror nuclei

Isospin symmetry:

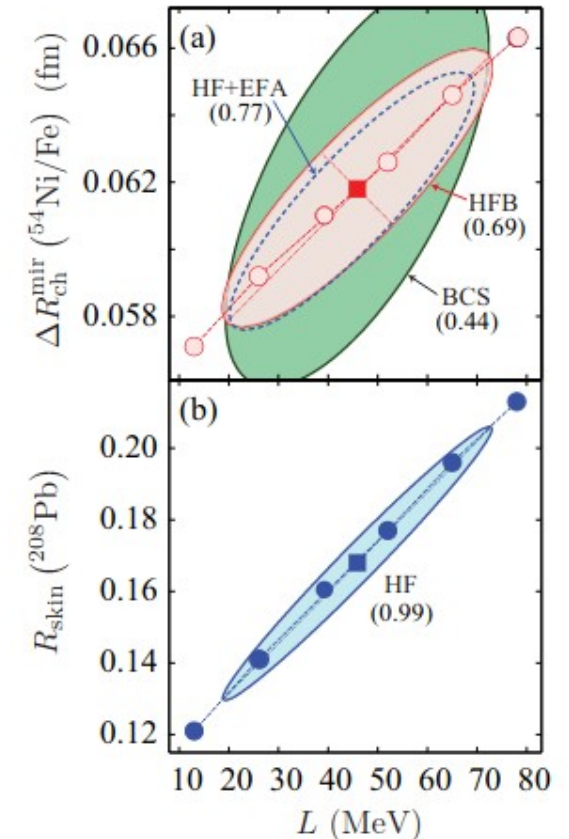
$$\Delta R_{np} = R_{ch}(^A_Z X_N) - R_{ch}(^A_N Y_Z) = \Delta R_{ch},$$



PHYSICAL REVIEW RESEARCH **2**, 022035(R) (2020)



PHYSICAL REVIEW C **105**, L021301 (2022)



Large theoretical uncertainties due to pairing correlations in the presence of low-lying proton continuum

Isvector giant resonances

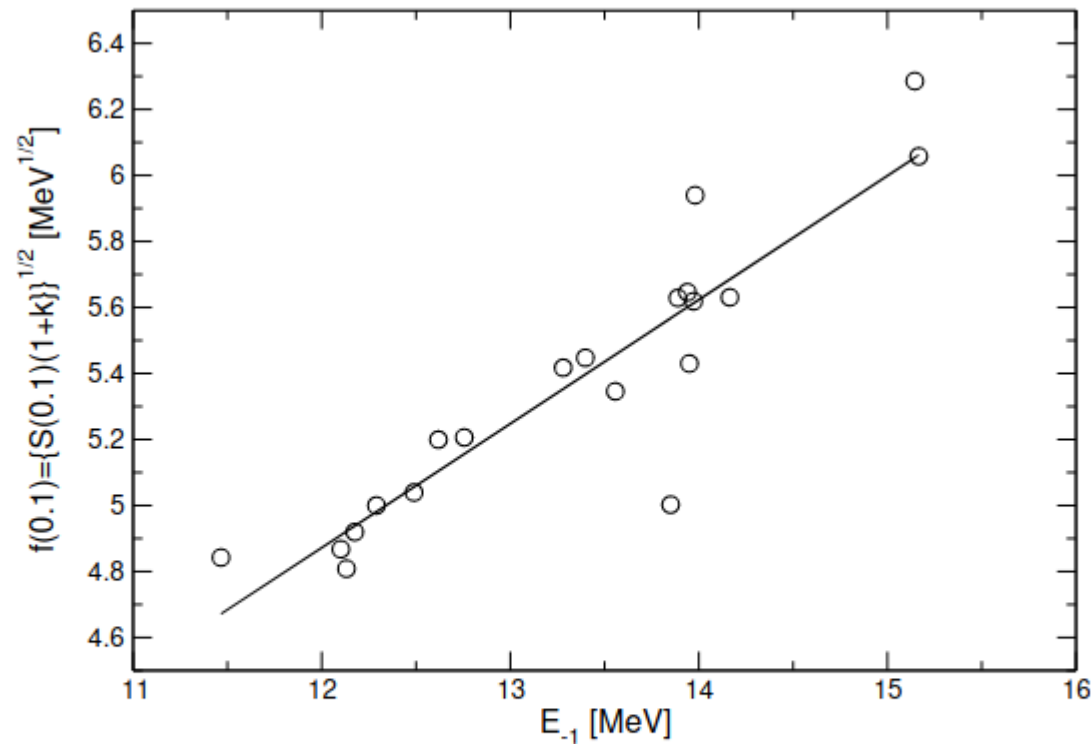
- In **isovector** giant resonances **neutrons and protons** “oscillate” out of phase
- **Isvector** resonances will depend on oscillations of the density $\rho_{iv} \equiv \rho_n - \rho_p \Rightarrow S(\rho)$ will drive such “oscillations”
- The **excitation energy** (E_x) within a **Harmonic Oscillator** approach is expected to depend on the symmetry energy:

$$\omega = \sqrt{\frac{1}{m} \frac{d^2U}{dx^2}} \propto \sqrt{k} \rightarrow E_x \sim \sqrt{\frac{\delta^2 e}{\delta \beta^2}} \propto \sqrt{S(\rho)}$$

where $\beta = (\rho_n - \rho_p) / (\rho_n + \rho_p)$

Giant Dipole Resonance

$$(E_x \approx f(0.1) \propto \sqrt{S(0.1 \text{fm}^{-3})})$$



Physical Review C 77, 061304 (2008)

The larger the symmetry energy at an average density of a finite heavy nucleus, the larger the excitation energy of the Giant Dipole Resonance (GDR).

Giant Quadrupole Resonance

X. Roca-Maza, M. Brenna, B. K. Agrawal, P. F. Bortignon, G. Colò, Li-Gang Cao, N. Paar, and D. Vretenar
 Phys. Rev. C **87**, 034301 – Published 1 March 2013

Within the Quantum Harmonic Oscillator approach

$$E_x^{IV} = 2\hbar\omega_0 \sqrt{1 + \frac{5\hbar^2}{42m} \frac{V_{\text{sym}} \langle r^2 \rangle}{(\hbar\omega_0)^2 \langle r^4 \rangle}}$$

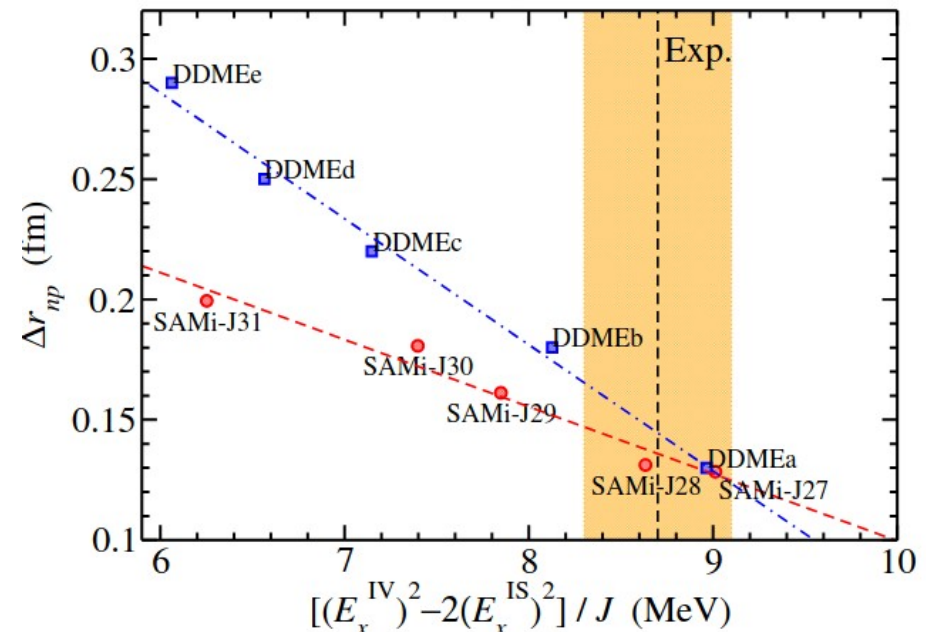
and EDF calculations, one can deduce

$$V_{\text{sym}} \approx 8(S(\rho_A) - S^{\text{kin}}(\rho_0))$$

$$S^{\text{kin}}(\rho_0) \approx \varepsilon_{F_0}/3 \text{ (Non-Rel)}$$

$$S(\rho_A) \approx J - L \frac{\rho_0 - \rho_A}{3\rho_0} \approx \frac{\varepsilon_{F_0}}{3} \left\{ \frac{A^{2/3}}{8\varepsilon_{F_0}^2} \left[(E_x^{IV})^2 - 2(E_x^{IS})^2 \right] + 1 \right\}$$

The larger the neutron skin in ^{208}Pb , the smallest the difference between the IS and IV excitation energies in GQRs.

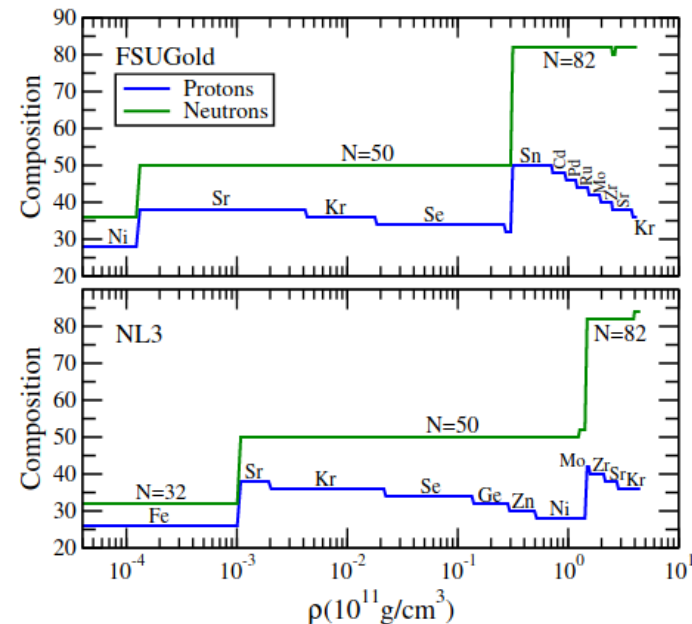


Implications for nuclear astrophysics from precision neutron skin measurements

- **Composition of the crust of a neutron star**
- **Mass-Radius relation of a neutron star**
- **Deformability of a neutron star**
- **Among other neutron star properties and astrophysical processes ...**

Outer crust of a neutron star (sub-saturation densities relevant)

- span 7 orders of magnitude in **density** (from **ionization** $\sim 10^4$ g/cm to the **neutron drip** $\sim 10^{11}$ g/cm)
 - it is organized into a **Coulomb lattice** of neutron-rich nuclei (ions) embedded in a relativistic **uniform electron gas**
 - $T \sim 10^6$ K ~ 0.1 keV → one can treat **nuclei and electrons at $T = 0$ K**
 - At the **lowest densities**, the electronic contribution is negligible so the Coulomb lattice is populated by ^{56}Fe nuclei.
 - As the **density increases**, the electronic contribution becomes important, it is energetically advantageous to lower its electron fraction by $e^- + (N, Z) \rightarrow (N + 1, Z - 1) + \nu_e$ and therefore $Z \downarrow$ with constant (approx) number of N
 - As the **density continues to increase, penalty energy from the symmetry energy** due to the neutron excess changes the composition to a different **N -plateau**
- $$\frac{Z}{A} \approx \frac{Z_0}{A_0} - \frac{P_{Fe}}{8a_{\text{sym}}}$$
- where $(A_0, Z_0) = ^{56}\text{Fe}_{26}$
- The Coulomb lattice is made of more and more neutron-rich nuclei until the critical **neutron-drip density is reached** ($\mu_{\text{drip}} = m_n$).
 $[M(N, Z) + m_n < M(N + 1, Z)]$

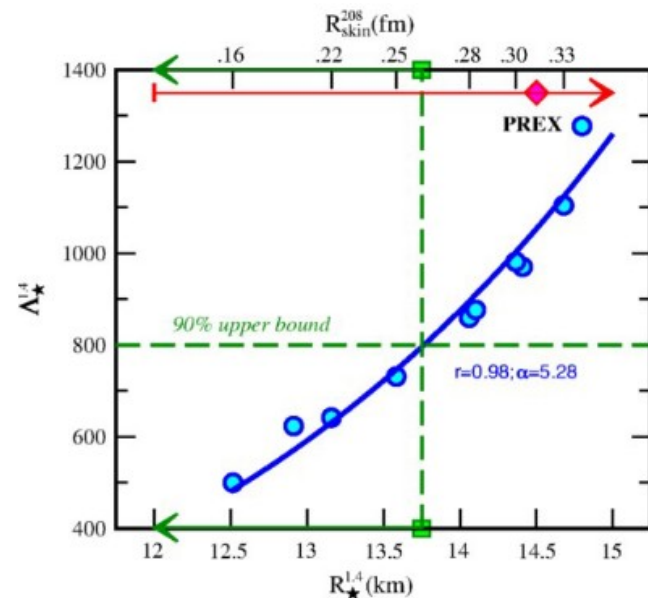
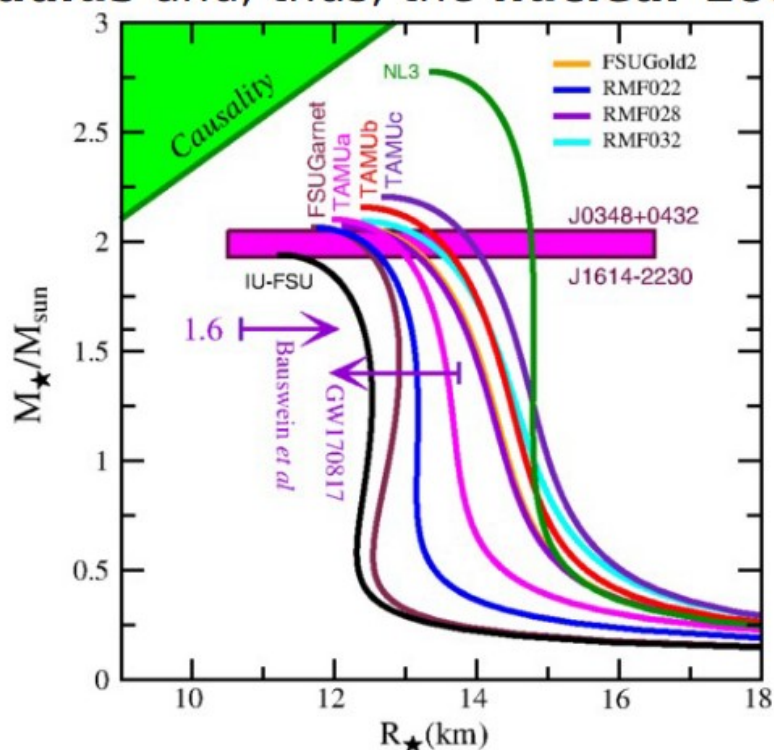


Physical Review C 78, 025807 (2008)

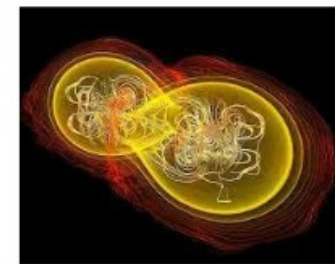
The larger the neutron skin of ^{208}Pb ($L \uparrow$), the more exotic the composition of the outer crust.

Mass-Radius relation and deformability of a Neutron Star

GW170817 from the binary neutron star merger → **constraint** neutron star **radius** and, thus, the **nuclear EoS**

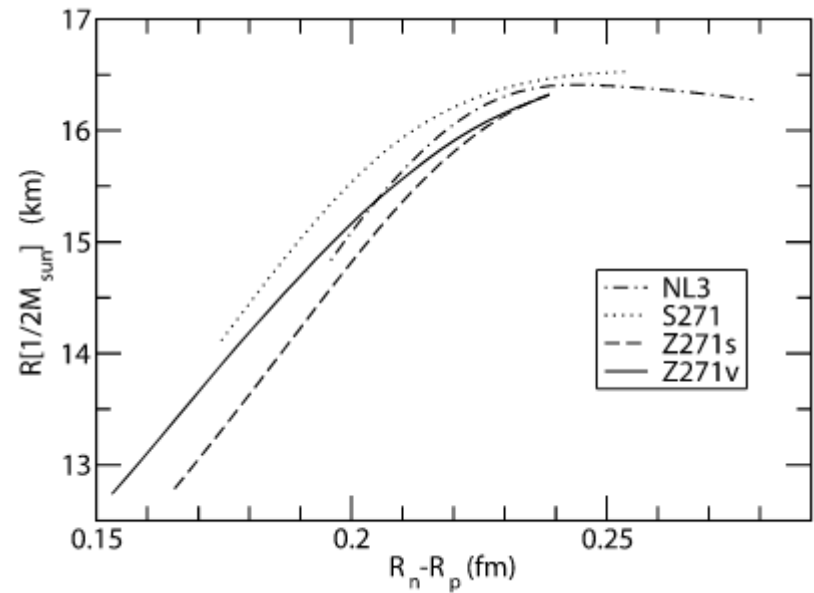
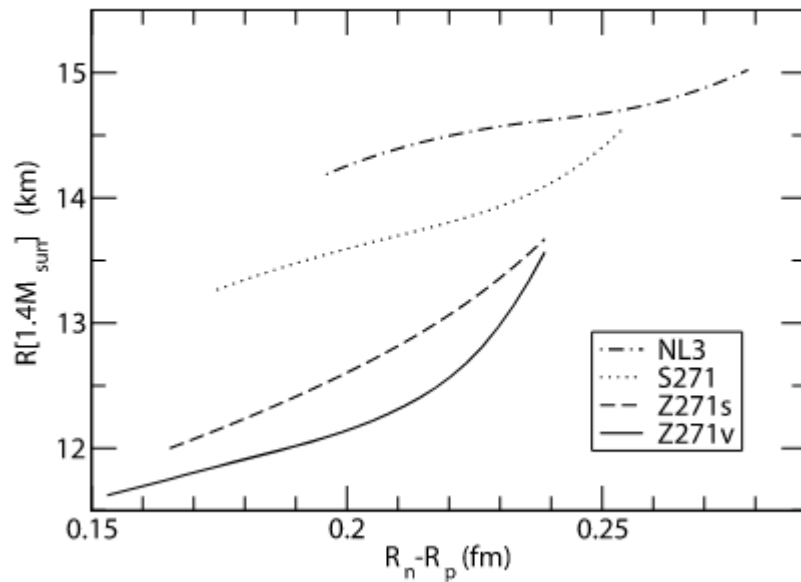


Tidal deformability (Λ) is a quadrupole deformation inferred from **GW signal** → proportional to **restoring force**. Hence, sensitive to the **nuclear EoS**



Neutron Skins and Neutron Stars in the Multimessenger Era
 F.J. Fattoyev, J. Piekarewicz, and C.J. Horowitz *Phys. Rev. Lett.* 120, 172702 (2018)

Radius of a Neutron Star



J. Carriere et al 2003 *ApJ* 593 463

Crust-core interface

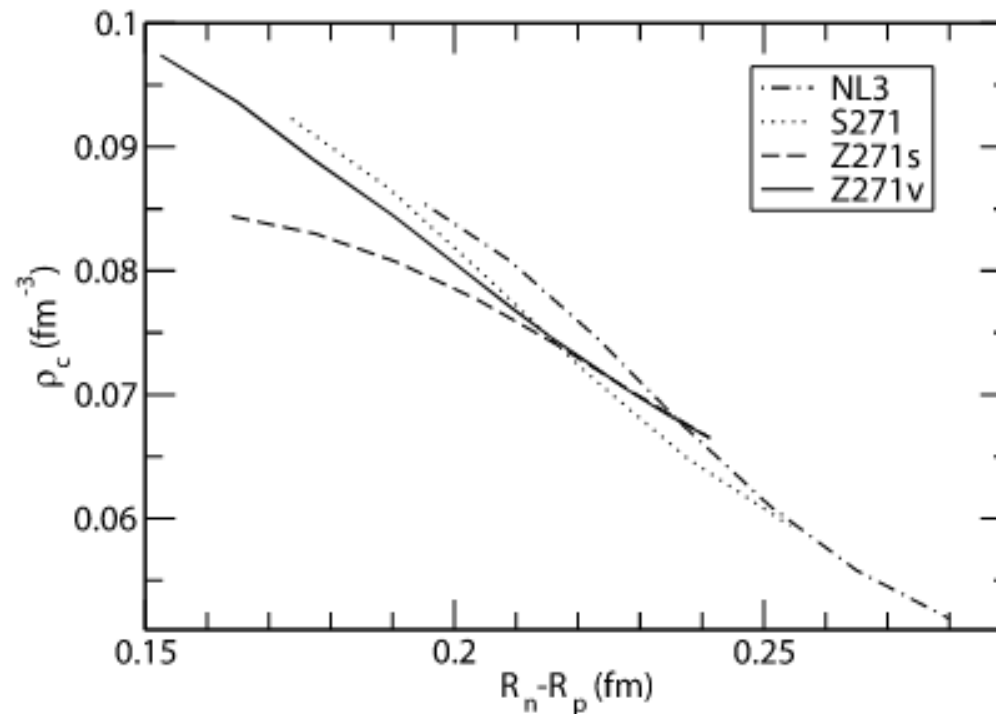


FIG. 1.—Transition density ρ_c at which uniform matter becomes unstable to density oscillations as a function of the neutron skin in ^{208}Pb . The solid curve is for the Z271 parameter set with $\Lambda_v \neq 0$ while the dashed curve uses Z271 with $\Lambda_s \neq 0$. The dotted curve is for the S271 set and the dot-dashed curve for NL3, both of these with $\Lambda_v \neq 0$.

J. Carriere *et al* 2003 *ApJ* **593** 463

THANK YOU!